



## The way forward, enhanced characterization of therapeutic antibody glycosylation: Comparison of three level mass spectrometry-based strategies

Elsa Wagner-Rousset<sup>a,\*</sup>, Audrey Bednarczyk<sup>b</sup>, Marie-Claire Bussat<sup>a</sup>, Olivier Colas<sup>a</sup>, Nathalie Corvaia<sup>a</sup>, Christine Schaeffer<sup>b</sup>, Alain Van Dorselaer<sup>b</sup>, Alain Beck<sup>a,\*</sup>

<sup>a</sup> Centre d'Immunologie Pierre Fabre, 5 Avenue Napoléon III, 74160 Saint-Julien-en-Genevois, France<sup>1</sup>

<sup>b</sup> Laboratoire de Spectrométrie de Masse Bio-Organique, Institut Pluridisciplinaire Hubert Curien IPHC-DSA, ULP, CNRS, UMR 7178, ECPM, 25 rue Becquerel, 67087 Strasbourg, France

### ARTICLE INFO

#### Article history:

Received 26 October 2007

Accepted 29 March 2008

Available online 15 April 2008

#### Keywords:

Therapeutic monoclonal antibodies

NS0 and CHO cell lines

Glycosylation

Oligosaccharides

N-glycans

Glycopeptides

Mass spectrometry

Tandem mass spectrometry

LC-ESI-TOF

RP-HPLC

LC-MS

NanoLC-Chip

Graphitized carbon

### ABSTRACT

Glycosylation which plays a crucial role in the pharmacological properties of therapeutic monoclonal antibodies (MAbs) is influenced by several factors like production systems, selected clonal population and manufacturing processes. Efficient analytical methods are therefore required in order to characterize glycosylation at different stages of MAbs discovery and production. Three mass spectrometry (MS)-based strategies were compared to analyze N-glycosylation of MAbs either expressed in murine myeloma (NS0) or Chinese Hamster Ovary (CHO) cell lines, the two current main production systems used for therapeutic MAbs. First a top-down approach was used on intact and reduced MAbs by liquid chromatography coupled to an electrospray ionization-time of flight mass spectrometer (LC-ESI-TOF), which provided fast and accurate profiles of MAbs glycosylation patterns for routine controls. Secondly, after digestion of the antibody with the peptide N-glycosidase F (PNGase F) enzyme, released N-linked glycans were directly analyzed by electrospray ionization-tandem mass spectrometry (ESI-MS/MS) without any prior derivatization, which gave precise details on the structure of the most abundant glycoforms. Finally, a bottom-up approach on tryptic glycopeptides using a nanoLC-Chip-MS/MS ion trap (IT) system equipped with a graphitized carbon column was investigated. Data were compared to those obtained with a more classical C18 reversed phase column showing that this last method is well suited to detect low abundant glycoforms and to provide in one shot information regarding both the oligosaccharide structure and the amino acid sequence of its peptide moiety.

© 2008 Elsevier B.V. All rights reserved.

### 1. Introduction

In the field of therapeutic recombinant proteins, monoclonal antibodies (MAbs) have achieved a rising success with at least 24 market approvals since 1986. This class of human drug is the fastest growing family with hundreds of MAbs in pre-clinical development and clinical trials [1]. One of their strengths is their higher success rate from clinical phase I to regulatory approval than for small-molecule drugs (25–29% versus 11%) [2,3]. Most of these MAbs belong to the class of immunoglobulin G (IgG), which are large homodimers of 150 kDa consisting in two light chains (LCs) and two heavy chains (HCs) connected by disulfide bonds to form a Y-

shaped structure. IgGs are serum proteins involved in the humoral immune response by binding specifically to target antigens. This binding consequently triggers either direct neutralization of the antigen, activation of the complement cascade or stimulation of effector cells via Fc receptor binding to the Fc region of the antibody.

One of the most important post-translational modification, affecting antibodies is by far glycosylation. Indeed mammal IgGs contain 2–3% carbohydrate by mass. A large majority of MAbs have only one N-linked glycosylation site generally located at Asn-297 in each heavy chain C<sub>H</sub>2 domain of the Fc portion [4]. N-linked glycosylation in the hypervariable regions of Fab domains has also been described, more often in human than murine IgGs (0.8% versus 0.3% in proportion by mass) [5]. Their occurrence and position are dependant on the presence of the consensus sequence Asn-Xaa-Thr/Ser (Xaa different from Pro).

Most licensed therapeutic MAbs are expressed in Chinese Hamster Ovary (CHO) cell lines or in murine myeloma NS0 or SP2/0 cells. In such cell lines, N-linked glycans are core fucosylated bi-antennary structures with more or less terminal galactosylations [6]. Therefore, recombinant MAbs consist of heterogeneous

\* Corresponding authors at: Centre d'Immunologie Pierre Fabre, Physico-Chemistry, 5 Avenue Napoléon III, BP 60497, 74160 Saint-Julien-en-Genevois, France. Tel.: +33 450356567; fax: +33 450353590.

E-mail addresses: [elsa.wagner@pierre-fabre.com](mailto:elsa.wagner@pierre-fabre.com) (E. Wagner-Rousset), [alain.beck@pierre-fabre.com](mailto:alain.beck@pierre-fabre.com) (A. Beck).

<sup>1</sup> [www.cipf.com](http://www.cipf.com).

mixtures of G0F (no galactosylation), G1F and G2F (one or two terminal galactoses, respectively) glycoforms. The proportion of each glycoform and the presence of atypical glycosylation types strongly depends on the producing cell lines and may differ significantly from natural human antibodies [7]. For example,  $\alpha$ -galactose and *N*-glycolylneuraminic acid (NGNA) moieties linked to the terminal galactose occur only in mouse cell lines and not in CHO [8]. In contrast, human IgGs contain oligosaccharides with *N*-acetylneuraminic acids (NANA). Moreover, bisecting *N*-acetylglucosamine (GlcNAc) containing oligosaccharides which represent up to 10% of the human IgG glycan population are uncommon in murine and CHO-derived antibodies [9–11]. Comparison between *N*-glycan structures on IgG Fab and Fc showed that glycosylation is site specific with higher extents of galactosylation and higher incidence of sialylated structures on Fab oligosaccharides [12].

Glycosylation of MAbs directly impacts on their biological activity whose mode of action involves effector function [13]. Whereas Fab glycosylation may affect binding affinity of the antigen, Fc glycosylation influences the structure and function of IgGs. Effector functions as well as immunogenicity and clearance are closely dependant on the glycosylation profile of MAbs [14,15]. Thus, the design of MAbs by glyco-engineering is a promising way to improve their clinical potency [16–20]. The process of glycosylation is not only influenced by the choice of the IgG production system but also by the cell culture conditions and clone selection [21]. Under non-optimal conditions, CHO, NS0 and SP2/0 cells can produce abnormally glycosylated products that lack *in vivo* efficacy or are potentially immunogenic in human [6]. That is why a careful selection of single cell clone and optimization of cell culture conditions are crucial steps to produce high quality recombinant IgGs (r-IgGs). However, discrepancies may still occur in the glycosylation profile for single cell clones from the same cell line. Consequently, at each step of MAb research, development and production, analytical controls are required to establish product integrity. It is also essential to determine the degree of heterogeneity due to post-translational modifications in order to ensure product consistency for comparability during process changes and scaling-up.

In the panel of available analytical methods, mass spectrometry (MS) has become a key technique to extensively characterize MAbs before therapeutic use in humans [22,23]. Well-established strategies for the structural analysis of glycoproteins and *N*-linked glycans have been described [24]. Their application to the detailed characterization of MAb glycosylation are presently either single or multi-methodological-based approaches [25–27]. These approaches can be classified according to two distinct levels, namely “top-down and bottom-up approaches”. The first strategy includes the analysis of intact or reduced MAbs, resulting in heavy and light chains then separable by chromatography. The second approach corresponds to the MS analysis of peptides after enzymatic digestion of the protein.

As a part of research and pre-clinical development of new therapeutic antibodies, we report and discuss herein the complementarities of different MS-based approaches for characterization of MAb glycosylation. According to the previously mentioned classification, a combination of three level techniques was investigated. The first one consists of the LC–MS analysis of intact or reduced MAbs using an electrospray-ionization time-of-flight analyzer (ESI-TOF). The second is a glycomics strategy with the structural characterization of released *N*-glycans by ESI-MS/MS. The final approach deals with peptide mapping and characterization by a novel nanoLC–Chip–MS/MS approach including glycopeptides enrichment and separation on a graphitized carbon column. Following a previous study [28], humanized MAbs expressed either in CHO or in NS0 cell lines as well as their murine hybridoma

counterpart were analyzed. In order to illustrate the utility of each approach, the diversity of glycosylation profiles are then compared and discussed.

## 2. Experimental

### 2.1. Material

All chemicals and reagents were of analytical grade and purchased from Sigma–Aldrich (Saint-Quentin Fallavier, France) or VWR International (Fontenay-sous-Bois, France). Distilled water produced from a Milli-Q Water System™ (Millipore, Guyancourt, France) was used for the preparation of the sample solutions.

### 2.2. Recombinant humanized and mouse antibodies

The recombinant antibodies analyzed in this study were expressed in eukaryotic cell lines at the Centre d'Immunologie Pierre Fabre (Saint Julien-en-Genevois, France) and purified using standard manufacturing procedures as previously described [28]. Humanized antibodies A2CHM and A3BHM were purified from CHO and NS0 cell supernatants respectively, whereas 7C10 was purified from a murine hybridoma.

### 2.3. Sample preparation

#### 2.3.1. Reduction and alkylation of MAbs

Twenty microgram of MAb was lyophilized and solubilized in 60  $\mu$ l Tris–HCl 100 mM, 2 mM EDTA, guanidine HCl 6 M, pH 8.0 buffer. Samples were flushed with  $N_2$ . Disulfide reduction was performed by incubating the MAb solution with 20 mM DTT (Sigma–Aldrich) for 2 h at 37 °C. Alkylation of cysteins was performed by adding 25 mM iodoacetamide (Sigma–Aldrich), the reaction occurred in the dark at room temperature within 1 h. The reaction was quenched by addition of acetic acid and *n*-propanol (final concentration 10 and 20%, respectively) either before or after alkylation depending on the experiments.

#### 2.3.2. Desalting the mixture of light and heavy chains prior to tryptic digestion

Reduced and alkylated LC and HC were desalted using a Zorbax 300SB-C8 Rapid Resolution Cartridge™, 2.1 mm  $\times$  30 mm, 3.5  $\mu$ m (Agilent Technologies, Massy, France) maintained at 60 °C. Mobile phase A consisted of acidified water (0.05% trifluoroacetic acid (TFA)) and solvent B was *n*-propanol:water, 90:10 containing 0.1% formic acid (HCOOH). The flow rate was set at 0.25 ml/min. After a 5 min desalting step at 100% A, an isocratic elution was performed at 70% B for 5 min. The elution of the fraction of interest was monitored at 280 nm. The LC and HC mixture was collected and lyophilized.

#### 2.3.3. Separation of light and heavy chains by SEC

MAb heavy and light chains were separated on a size-exclusion column and the corresponding fractions were collected and concentrated as previously described [28].

#### 2.3.4. Tryptic digestion

Either alkylated HC or a mixture of alkylated HC and LC (~80  $\mu$ g) was solubilized with 100  $\mu$ l Tris–HCl 50 mM, 1 mM  $CaCl_2$ , pH 7.5 buffer. 10  $\mu$ l of Rapidigest™ (Waters, Saint Quentin-en-Yvelines, France) 1% in aqueous solution were added in order to speed up the enzymatic reaction. Digestion was performed by adding 10  $\mu$ l of a trypsin solution ( $c = 0.5 \mu$ g/ $\mu$ l in water) (Trypsin Sequencing Grade™, Roche Diagnostics, Meylan, France), which corresponds

to a 1:16 ratio enzyme:substrate. Samples were incubated at 37 °C for 2 h. The reaction was stopped by adding 0.4 µl TFA.

#### 2.3.5. Release and purification of N-glycans

Glycans were released from MABs by incubation with 3 µl of PNGase F ( $5 \times 10^5$  U/ml, New England Biolabs, Hitchin, UK) per mg of glycoproteins in their initial buffer, overnight at 37 °C. For desalting and purification we used Carbograph™ cartridges (Alltech, Goussainville, France). N-glycans were eluted from the cartridges within 1 ml of a solution containing acetonitrile:water (70:30)+0.02% TFA. Before being infused in the ion trap (IT), the solution was first diluted 10 times with acetonitrile:water (50:50)+0.1% HCOOH.

#### 2.4. LC-ESI-TOF experiments

The high performance liquid chromatography (HPLC) system used in this study consisted of a Waters Alliance™ 2695 separation module equipped with a column-heating compartment and a 996™ photodiode array detector (Waters, Saint-Quentin-en-Yvelines, France). All LC-MS experiments performed with this system were running at 0.25 ml/min. The flow rate was not split for MS detection. Mass spectrometric analysis was carried out in W positive ion mode on a Waters LCT Premier™ equipped with an ESI source (Waters, Saint-Quentin-en-Yvelines, France). The source and desolvation temperatures were set at 120 and 300 °C, respectively. The nitrogen gas flow rates were set at 50 l/h for the cone and 350 l/h for desolvation. Calibration was carried out using a 2 µg/µl solution of cesium iodide (Sigma-Aldrich) for the protein mass measurements. MS data were acquired and processed using MassLynx™ 4.1 (Waters). Deconvolution of the protein mass spectra was performed with Transform™ (Waters). Standard deviations for mass measurements were those given by treatment of the multiply charged ion spectrum using Mass Lynx™.

##### 2.4.1. LC-MS of intact MABs

Ten micrograms of intact or deglycosylated antibody were loaded onto a Zorbax™ 300SB-C8 Rapid Resolution Cartridge™, 2.1 mm × 30 mm, 3.5 µm (Agilent Technologies, Massy, France) maintained at 60 °C. The protein was first rinsed on the cartridge for 20 min with 90% solvent A (water + 0.02% TFA and 1% HCOOH), 10% solvent B (water:n-propanol, 10:90 + 0.02% TFA and 1% HCOOH). Elution was then performed using an isocratic step consisting of 50% of B for 10 min followed by a 10 min step washing at 80% B and by a final equilibration period of 10 min at 10% B. Capillary and cone voltages were optimized for maximum sensitivity at each experiment. Ion guide one and Aperture 1 voltages were both set at 40 V.

##### 2.4.2. LC-MS of reduced MABs

Five micrograms of reduced antibody were loaded onto an Agilent Zorbax™ 300SB-C8 column, 2.1 mm × 150 mm, 3.5 µm (Agilent Technologies, Massy, France) maintained at 60 °C. Proteins were eluted from the column using a linear gradient from 20 to 35% of B in 30 min (solvent A = water + 0.02% TFA and 1% HCOOH; solvent B = water:n-propanol, 10:90 + 0.02% TFA and 1% HCOOH). The column was then flushed with 80% B for 5 min followed by an equilibration step of 10 min at 20% B. Capillary and cone voltages were optimized for maximum sensitivity at each experiment. Ion guide one and Aperture 1 voltages were set at 20 and 30 V, respectively.

#### 2.5. ESI-MS/MS of released N-glycans

MS/MS experiments on N-glycans were performed with an Esquire 3000+™ ion trap (Bruker Daltonics, Bremen, Germany)

equipped with an electrospray ion source working in positive mode. The sample solutions were infused at 4 µl/min with a syringe pump. The voltage applied to the counter electrode was set at 4000 V. The voltage on the metal glass capillary interface was optimized at 225 V and the voltage applied to the skimmer was set at 40 V. For tandem mass experiments, the precursor ions were fragmented applying a resonance frequency on the end cap electrodes (peak-to-peak amplitude 0.8 V) matching to the frequency of the selected ions. Fragmentation of the precursor ions occurred in the ion trap due to collisions with helium gas buffer (pressure 5 mPa). Scanning was performed in standard resolution mode at a scan rate of 13,000 *m/z* per second. A total of 50 scans were averaged to obtain a mass spectrum. Calibration of the ion trap was performed using ions from a Tuning Mix™ solution (Bruker Daltonics) over mass range from *m/z* 100 to 1800.

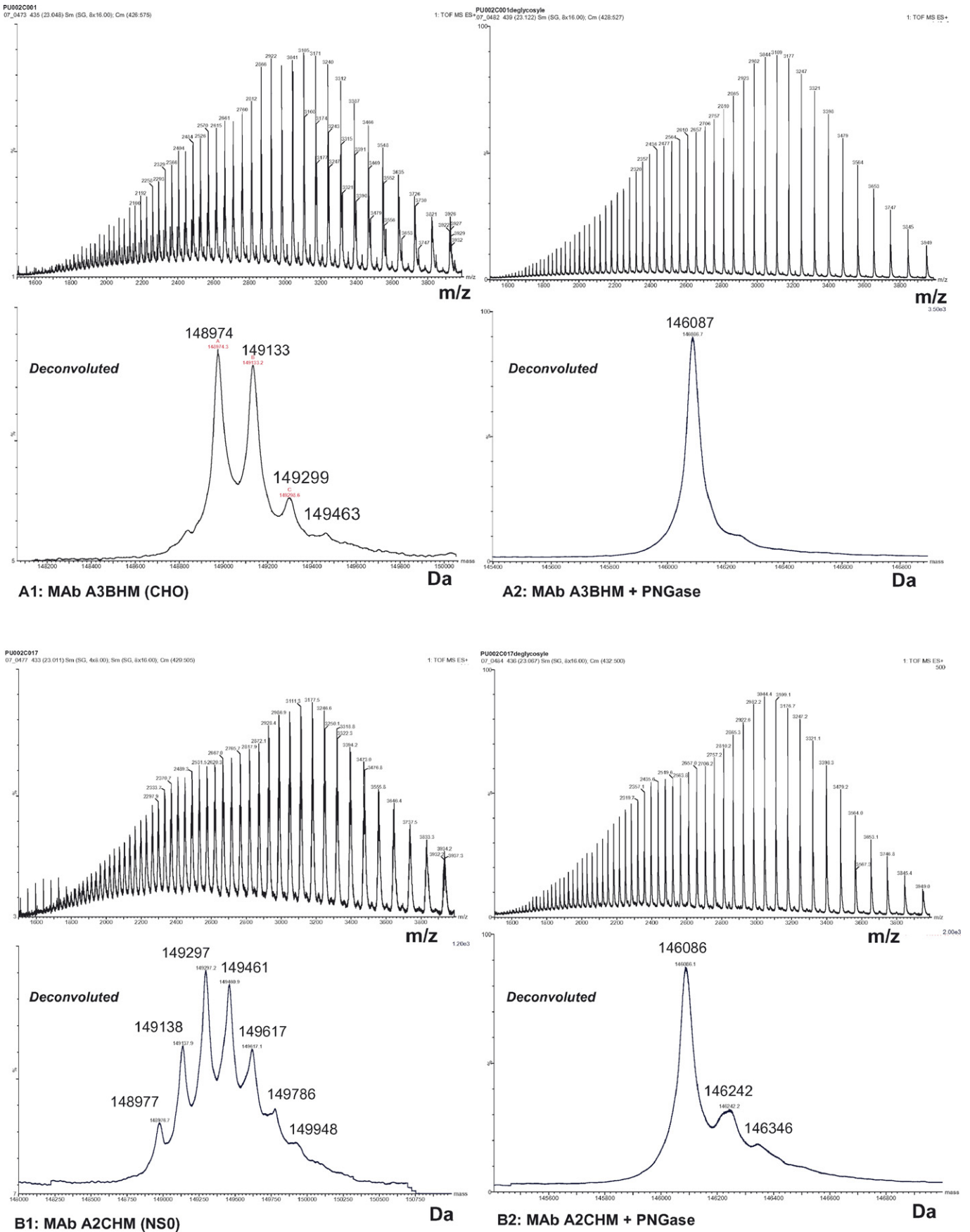
#### 2.6. NanoLC-Chip-MS/MS experiments

NanoLC-MS/MS analysis of the tryptic digest was performed using an Agilent 1100 series HPLC-Chip system™ (Agilent Technologies, Palo Alto, USA) coupled to an HCTplus™ ion trap (Bruker Daltonics). Chromatographic separations were performed using three columns: a 43 mm × 75 µm, 5 µm reversed phase C18 column, a 150 mm × 75 µm, 5 µm reversed phase C18 column and a 43 mm × 75 µm, 5 µm porous graphitized carbon column. The same chromatographic conditions were used for the three analysis types with a gradient going from 3 to 20% in 10 min and from 20 to 35% of eluant B in 30 min with A: water + 2% acetonitrile + 0.1% HCOOH and B: acetonitrile + 2% water + 0.1% HCOOH, at a flow rate of 300 nl/min. The voltage applied to the capillary cap was set to 1750 V in order to avoid glycopeptides *in-source* fragmentation. No oxonium ions such as [HexNAc + H]<sup>+</sup> or [HexHexNAc + H]<sup>+</sup> ions at *m/z* 204 or 366, signature of glycan fragmentations, were observed in the MS spectra. The mass spectrometer transmission parameters were optimized for high *m/z* set optimal around 1300 *m/z*. Using exclusion lists, MS/MS experiments were selectively performed in ranges of 4 *m/z* corresponding to the generated glycopeptide ions. The system was operated with automatic switching between MS and MS/MS modes. The three most abundant species of each *m/z* range were selected to be further isolated and fragmented. Fragmentation amplitude was set at 1 V. The MS/MS scanning was performed in the ultrascan resolution mode at a scan rate of 26,000 *m/z* per second. A total of three scans were averaged to obtain a MS/MS spectrum. The complete system was fully controlled by ChemStation™ (Agilent Technologies) and EsquireControl™ (Bruker Daltonics) softwares.

### 3. Results

#### 3.1. LC-ESI-TOF of intact and reduced MABs

Successful optimizations of analytical reversed phase-high performance liquid chromatography (RP-HPLC) methods have been made in the last 3 years in order to improve analysis of high molecular weight proteins and especially monoclonal antibodies [29,30]. Such approaches were then used as a starting point for the method development of chromatographic conditions providing efficient separation of light chain and multiple variants of heavy chains [31]. In parallel, the wide mass range of a TOF analyzer combined with high mass resolution and accuracy enable the fine structural characterization of MABs [22,32,33]. Mass accuracy in measuring different intact antibodies was shown to reach below 30 ppm ( $\pm 4$  Da) by using a 10,000 instrument resolution with an appropriate standard antibody as external calibration agent [34].



**Fig. 1.** Positive ion ESI mass spectra of monoclonal antibodies (A) A3BHM, (B) A2CHM either intact (1) or treated with PNGase F (2). Multiply charged ions spectra are shown at the top whereas the result of deconvolution presenting the molecular mass of the antibody is shown below.

**Table 1**  
MABs isoforms mass assignment after LC–ES–TOF analysis (see spectra Fig. 1)

	Glycoforms	Measured masses (Da)	Calculated average mass (Da)	$\Delta$ Mass (Da)
Deglycosylated A3BHM	–	146,087 $\pm$ 3	146,087	0
A3BHM	G0F/G0F	148,974 $\pm$ 7	148,975	–1
	G0F/G1F	149,133 $\pm$ 6	149,137	–4
	G1F/G1F	149,299 $\pm$ 7	149,300	–1
	G0F/G2F			
	G1F/G2F	149,461 $\pm$ 14	149,462	–1
Deglycosylated A2CHM	–	146,086 $\pm$ 2	146,087	–1
	?	146,242 $\pm$ 30	–	156
	?	146,346 $\pm$ 16	–	260
	G0F/G0F	148,977 $\pm$ 11	148,975	+2
	G0F/G1F	149,138 $\pm$ 6	149,137	+1
	G1F/G1F	149,297 $\pm$ 6	149,300	–3
	G0F/G2F			
A2CHM	G1F/G2F	149,461 $\pm$ 6	149,462	–1
	G2F/G2F	149,617 $\pm$ 7	149,624	–7
	G2F/G2F + Gal	149,786 $\pm$ 16	149,786	0
	G2F/G2F + 2Gal	149,948 $\pm$ 19	149,948	0

Also, suitable RP–HPLC methods in conjunction with ESI–TOF–MS are now methods of choice for efficient analysis of intact or reduced antibody with minimal sample preparation [35]. Applicability of the LC–ESI–TOF approach for MABs analysis was demonstrated with efficient characterization of structural variants and degradation products [30,36]. RP–HPLC in combination with mass spectrometry was employed in order to address common modifications of therapeutic antibodies including formation of N-terminal pyroglutamate, C-terminal lysine variants and heterogeneous glycosylation profiles [29,35,37,38] as well as for the determination of minor modifications such, e.g. as tryptophan oxidation [39].

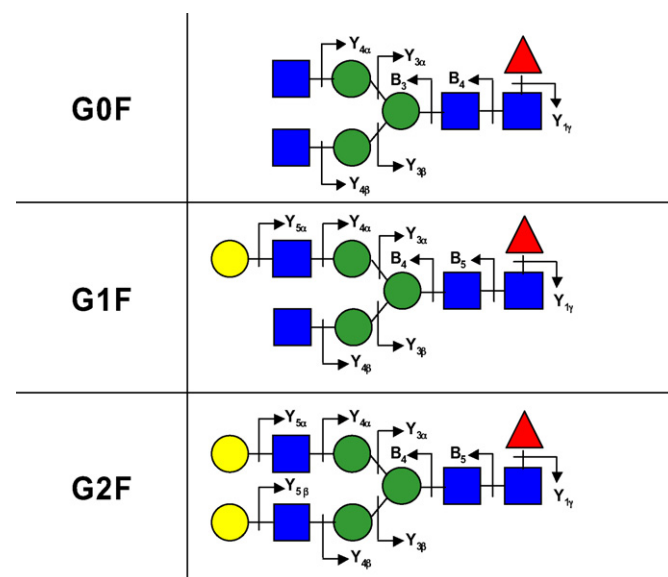
### 3.1.1. Monitoring glycosylation profile of intact MABs

Fig. 1 shows ESI mass spectra of two humanized monoclonal antibodies produced in different cell lines, either intact (Fig. 1A1 and B1) or treated with PNGase F (Fig. 1A2 and B2). The analysis gave spectra that consisted of typical series of multiply charged ions with  $m/z$  values ranging from 1500 to 4000  $m/z$ . The associated deconvoluted spectra are shown below. Assignment of the experimental masses (Table 1) was made by comparison with the calculated masses from the cDNA-derived amino acid sequence. MABs theoretical masses were calculated assuming 16 disulfide bridges, heavy chain N-terminal pyroglutamic acids formation ( $-2 \times 17$  Da) and C-terminal lysine clipping ( $-2 \times 128$  Da) expected for a humanized antibody IgG1 [40]. Masses of the most common N-glycans associated with the Fc domain of recombinant IgG1 [41] (see structures Fig. 2) were considered as part of post-translational modifications. In the case of deglycosylation (Fig. 1A2 and B2), Asn<sup>297</sup> changed into aspartic acid (Asp) in both heavy chains subsequently increasing the mass by 2 Da. Whereas A3BHM spectrum (Fig. 1A2) displays a single peak at 146,087  $\pm$  3 Da after deglycosylation, A2CHM spectrum (Fig. 1B2) exhibits two additional peaks at about  $m/z +156 \pm 30$  Da and  $+260 \pm 16$  Da. The wide shape and low intensity of those peaks make their measurement rather inaccurate and hence, their interpretation quite unclear. A first hypothesis to explain this heterogeneous profile would be the presence of two minor variants with addition of non-cleaved lysine (1 and 2 K) resulting in a theoretical positive mass shift of  $2 \times 128$  Da. Indeed, the cleavage of the C-terminal lysines which is due to the activity of carboxypeptidase B [42,42] could be incomplete. Another hypothesis would be the glycation occurring on N-terminus or lysine residue (162 Da mass shift). Glycation would result from the cell culture conditions and would be caused by the presence of glucose in cell culture media [43,44]. Mass spectra of the intact antibody,

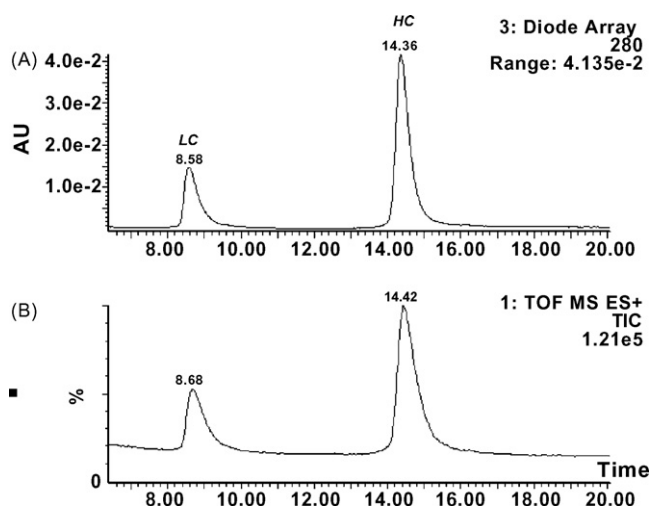
without PNGase F treatment, yield clear glycosylation profiles containing combinations of bi-antennary glycans with a variable number of galactose residues. Spectrum of A3BHM (Fig. 1A1) shows an heterogeneity corresponding to additional galactoses on the N-acetylglucosamines of the predominant G0F isoform. G1F and G2F glycoforms are typical of MAB expressed in CHO cell lines, without any terminal extended galactosylation. On the other hand, A2CHM spectrum (Fig. 1B1) exhibits a more complex distribution of glycoforms with at least seven peaks including minor structures possessing extended galactosylation ( $\alpha$ 1–3 Gal) which are characteristic of MAB produced in NS0 cell lines [45].

### 3.1.2. Monitoring glycosylation profile of the heavy and light chains

Another way to address antibody heterogeneity is to consider mass spectra of both individual heavy and light chains separated by RP–HPLC. Fig. 3 shows a typical chromatogram of reduced A2CHM



**Fig. 2.** Structures of the three most abundant N-glycans described in this study represented using the symbol nomenclature outlined by the consortium for functional glycomics (<http://www.functionalglycomics.org/>). (■) N-Acetylglucosamine, (●) mannose, (●) galactose and (▲) fucose. Main glycosidic fragments observed after MS/MS experiments are annotated.



**Fig. 3.** Reversed-phase chromatograms of the reduced forms of the monoclonal antibody A2CHM showing the separation of light and heavy chains (LCs and HCs) by LC-ES-TOF. (A) UV detection, signal extracted at 280 nm. (B) Corresponding total ion current.

obtained in LC-MS. Multiply charged ion spectra and deconvoluted mass spectra of light and heavy chains for two monoclonal antibodies are presented in Fig. 4 for comparison between humanized (A2CHM; Fig. 4A) and murine (7C10; Fig. 4B) antibodies. Whereas light chains of both MABs exhibit a main sharp peak accompanied by small probable salt adductions (Fig. 4A1 and B1), heavy chain spectra reflect the glycosylation heterogeneity profile of each IgG (Fig. 4A2 and B2). As already described for murine and CHO-expressed antibodies, minor glycoforms correspond to overgalactosylated N-glycans (G2F +  $\alpha$ 1-3 Gal and G2F + 2  $\alpha$ 1-3 Gal, see Table 2). The main difference between these two MABs remains in the proportion of each form. As G1F is the most abundant isoform for A2CHM, G0F and G1F are both predominant for the murine antibody.

### 3.1.3. Comparison between intact and reduced MAB mass measurements

Contrary to the direct mass measurement of intact antibody (150 kDa, mass range around 3000  $m/z$ ) carrying simultaneously two N-glycosylation sites, the analysis of reduced MAB allows to decrease the sample complexity linked to single N-glycosylation that occurs on both heavy chains of the IgG in an asymmetrical manner. Thus, the MAB reduction reduces the mass of the fragment of interest (heavy chain, 50 kDa, mass range around 1500 up to 2000  $m/z$ ) to a range where it is possible to get higher resolution mass spectra and accuracy which allows bet-

ter differentiation of glycoforms with close masses. The precision of these techniques was assessed by analysis of the calculated and measured masses with an average error range for the mass measurement within  $2 \pm 10$  Da for intact A2CHM,  $4 \pm 9$  Da for its heavy chain and  $0 \pm 1$  Da for its light chain. Finally, ESI-TOF data alone were sufficient for structural assignments of three main glycoforms plus two others related to micro-heterogeneous profiles.

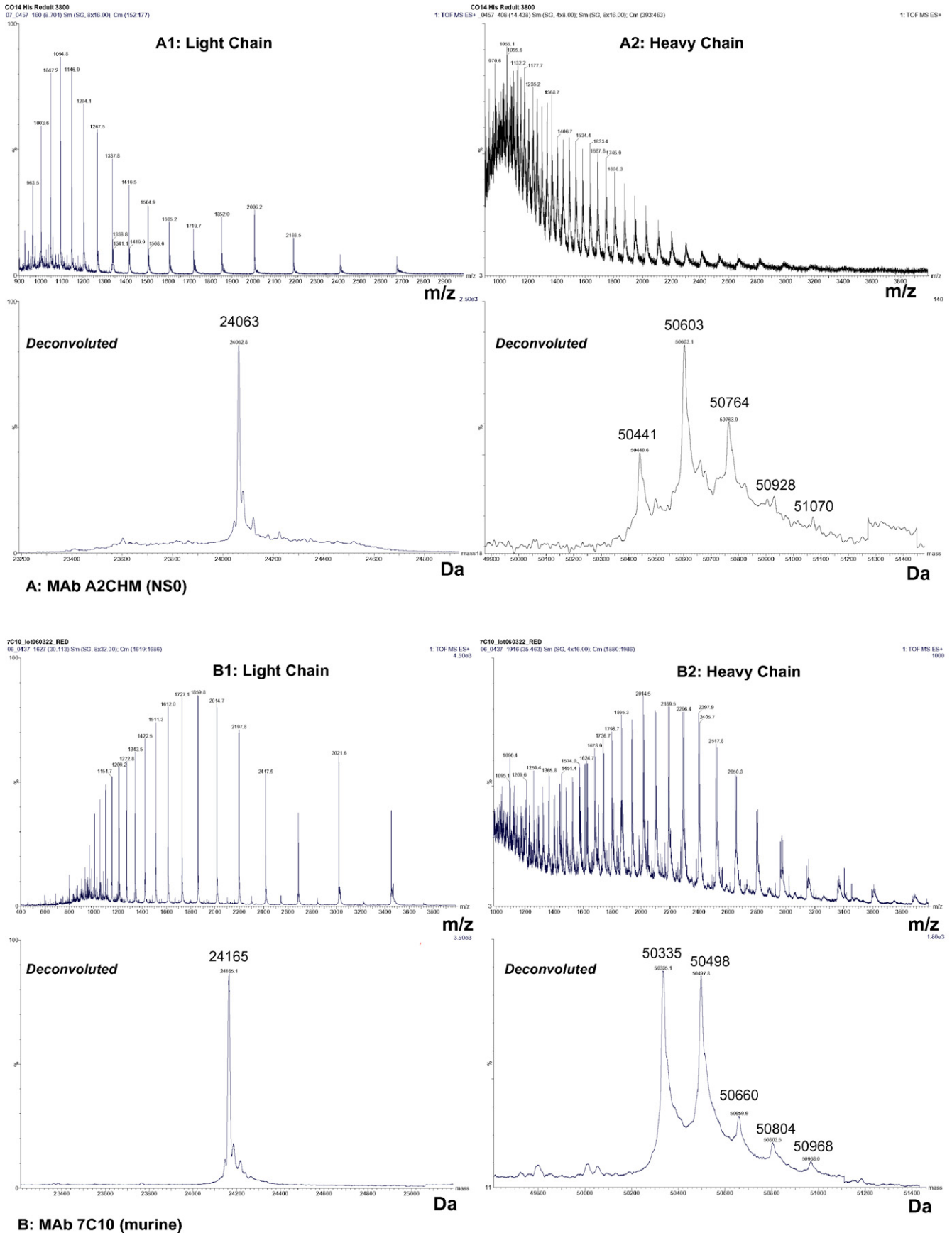
### 3.2. Direct analysis of released N-linked glycans by tandem mass spectrometry

Structural characterization of individual N-glycans is challenging due to their branched and isomeric nature [24]. Mass spectrometry has been widely used to successfully address this question. As glycans consist of a limited set of oligosaccharide moieties, a single mass measurement may sometimes be sufficient to deduce the monosaccharide composition. However, more sophisticated methods are required to determine linear sequences, branching and linkages. Additional information can be obtained by fragmentation analysis of isolated N-glycans by ESI-MS/MS with high or low collision-induced dissociation (CID) [46]. For that purpose, the ion trap mass spectrometer (ITMS) with its ability to perform multiple stages of fragmentation ( $MS^n$ ), is particularly useful and allows a fine characterization of carbohydrates [47,48]. The hydrophilic character of oligosaccharides is responsible for a decrease of their ionization efficiency and thus of a lack of sensitivity when analyzed by ESI. To circumvent this problem glycans can be derivatized or ionized as adducts of alkali metals [49,50]. The fragmentation pattern of underivatized  $[M+H]^+$  ions is less complex than one obtained with sodium or metal adducts. Whereas  $[M+H]^+$  ions produce mainly B and Y-type glycosidic fragments, adducts of alkali metals give additional fragments like cross-ring cleavages which can be informative but also greatly increases the complexity of spectra.

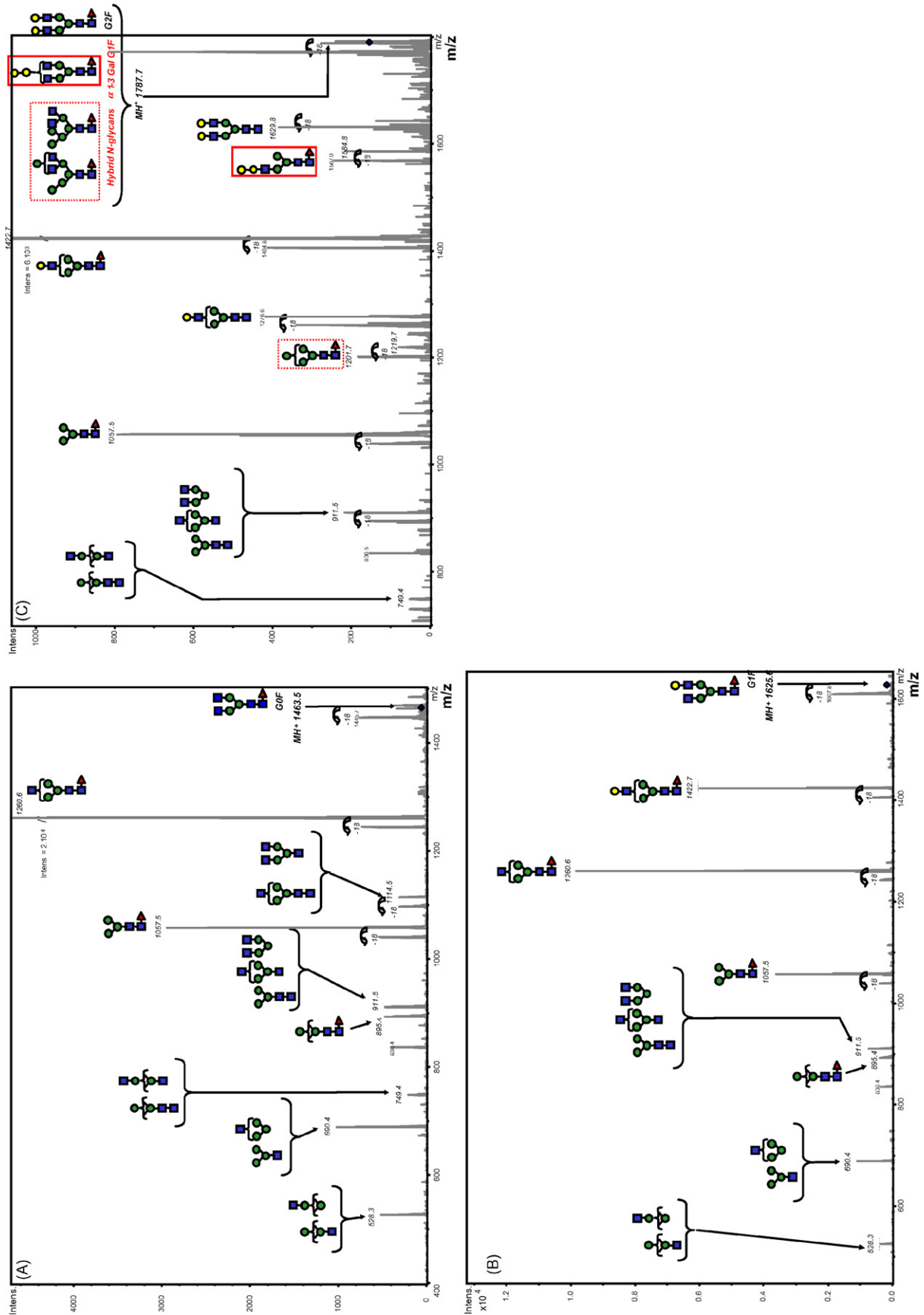
In the present work, we first released N-linked glycans from the monoclonal antibody A2CHM with the commercially available enzyme peptide N-glycosidase F (PNGase F). Glycans were then purified and desalted from the resulting mixture thanks to graphitized carbon cartridges. Mass spectrometry analysis was performed by infusion of the oligosaccharides solution into an ESI-ion trap without any prior separation. Parent ions corresponding to the protonated form  $[M+H]^+$  of the three main carbohydrate structures (G0F, G1F and G2F) were successively isolated and fragmented by  $MS^2$  in the analyzer. The interpretation of mass spectra was facilitated by the use of an *in-house* software which compiles glycan structures defined by users in order to calculate all the theoretical fragments resulting from one or several inter-glycosidic cleavages [51]. The glycan fragments are annotated according to the nomenclature of Domon and Costello [52]. Y and B series fragments

**Table 2**  
Heavy and light chains mass assignment after LC-ES-TOF analysis (see spectra Fig. 3)

	Glycoforms	Measured masses (Da)	Calculated average mass (Da)	$\Delta$ Mass (Da)
Light chain A2CHM	–	24,063 $\pm$ 1	24,063	0
	G0F	50,441 $\pm$ 5	50,441	0
Heavy chain A2CHM	G1F	50,603 $\pm$ 4	50,603	0
	G2F	50,764 $\pm$ 4	50,765	–1
	G2F + Gal	50,928 $\pm$ 10	50,927	+1
	G2F + 2Gal	51,070 $\pm$ 21	51,089	–19
Light chain 7C10	–	24,165 $\pm$ 1	24,165	0
	G0F	50,335 $\pm$ 4	50,334	+1
Heavy chain 7C10	G1F	50,498 $\pm$ 4	50,496	+2
	G2F	50,660 $\pm$ 6	50,658	+2
	G2F + Gal	50,804 $\pm$ 17	50,820	+16
	G2F + 2Gal	50,968 $\pm$ 20	50,982	+14



**Fig. 4.** Positive ion ESI mass spectra of light chains (1) and heavy chains (2) from reduced monoclonal antibody after chromatographic separation. (A) A2CHM and (B) 7C10. Multiply charge ions spectra are shown at the top whereas the result of deconvolution presenting the molecular mass of the antibody is shown below.



**Fig. 5.** Tandem mass spectra of glycans G0F (A), G1F (B) and G2F (C) isolated respectively at  $m/z$  1463.5, 1625.6 and 1787.7 by ES-ion trap. A structural interpretation of the fragmentation pattern is proposed and illustrated. (C) Both fragments in frames are related to parent ion structures which differ from G2F. The ion at  $m/z$  1219.7 may be originated from hybrid N-glycans isobaric with G2F. The fragment at 1567.0 is the signature of an  $\alpha$ -1-3 Gal-G1F isomer.



corresponding to the potential glycosidic cleavages of the isoforms G0F, G1F and G2F are presented in Fig. 2.

Fig. 5A displays the MS/MS spectrum for the N-glycan G0F. By collision with helium, the singly charged parent  $[M+H]^+$  ion ( $m/z$  1463.5) produces a large variety of ions resulting exclusively from glycosidic cleavages. The pattern of ions yields structural information consistent with the expected N-linked oligosaccharide structure. The parent ion and some fragments show a primary loss of a molecule of water ( $-18$ Da). The prominent ion at  $m/z$  1260.6 ( $Y_{4\alpha}$  or  $\beta$ ) is due to the loss of a single GlcNAc residue from the non-reducing terminus. The spectrum reflects two main fragmentation pathways. Within the first pathway, the Y ion series at  $m/z$  1260.6, 1057.5 and 895.4 conserves the core-fucosyl region intact and results in progressive loss of mannose from the non-reducing terminus. The second pathway, which generates smaller peaks, first triggers the loss of the fucosyl residue together with a GlcNAc ( $m/z$  1114.5). Several ions ( $m/z$  749.4, 690.4 and 528.3) are coincident in mass with multiple glycosidic cleavages and may be the result of both pathways. Such ions correspond to the internal fragments  $(Man)_2(GlcNAc)_2$ ,  $(Man)_3(GlcNAc)_1$  and  $(Man)_1(GlcNAc)_1$ , respectively. We were not able to see smaller fragments due to the low mass cutoff of the ion trap.

In Fig. 5B is represented the MS/MS spectrum of the N-glycan G1F. Fragmentation of this oligosaccharide follows the same pattern as previously described for G0F. By the main pathway, the core-fucosyl moiety is conserved and the non-reducing residues are progressively lost. Most of the fragments belonging to this pathway lose water. If compared to the G0F MS<sup>2</sup> spectrum, G1F presents more or less the same profile with an additional characteristic fragment ( $Y_{5\alpha}$ ), which carries the  $\alpha$ 1-3 Gal residue.

Finally, we performed MS/MS on the ion at  $m/z$  1769.9 (Fig. 5C), which is the calculated mass of the protonated N-glycan G2F. Once again, this experiment triggers fragments, which result from only one or several inter-glycosidic cleavages. Surprisingly, we found two masses that could not be deduced from the G2F structure. The first one at  $m/z$  1584.8 corresponds to the lack of one GlcNAc from the precursor ion ( $-203$ Da). This fragment may correspond to a certain proportion of an isomeric form of G2F which would be a G1F+ $\alpha$ 1-3 Gal form. This isobar of G2F triggers to the  $Y_{4\beta}$  fragment  $(Gal)_2(GlcNAc)_3(Man)_3(Fuc)_1$  at  $m/z$  1585. The second unexpected fragment ion was measured at  $m/z$  1219.7 and is interpreted as a loss of two GlcNAc plus one hexose from the precursor ion. This fragment is still fucosylated, which means that its reducing terminus part is intact. By considering possible combinations of sugars that could be added to the core heptasaccharide, two isomeric structures of G2F may theoretically lead to such a fragmentation (see Fig. 5C in frame) for a small portion of hybrid type N-glycans either tri or tetra-antennary. As the NS0 cell line used to produce A2CHM does not express the N-acetylglucosaminyltransferase III (GnTIII) that adds a bisecting GlcNAc residue [6], we did not consider this possibility. In summary, we proposed two hybrid N-glycans forms, which might result from an incomplete glycan maturation process in cells. A previous study using MS together with sequential enzymatic digestion has shown complete characterization of such low-amount N-linked glycans released from a murine MAb [25]. Also, additional experiments would help to discriminate between the isobaric forms of G2F. For example, the endoglycosidase H (Endo H) would cleave within the core of an hybrid structure but not of a complex one. Digestion with this enzyme followed by mass measurement would help to confirm the presence of hybrid N-glycans and eventually to determine the relative amount of each form [53].

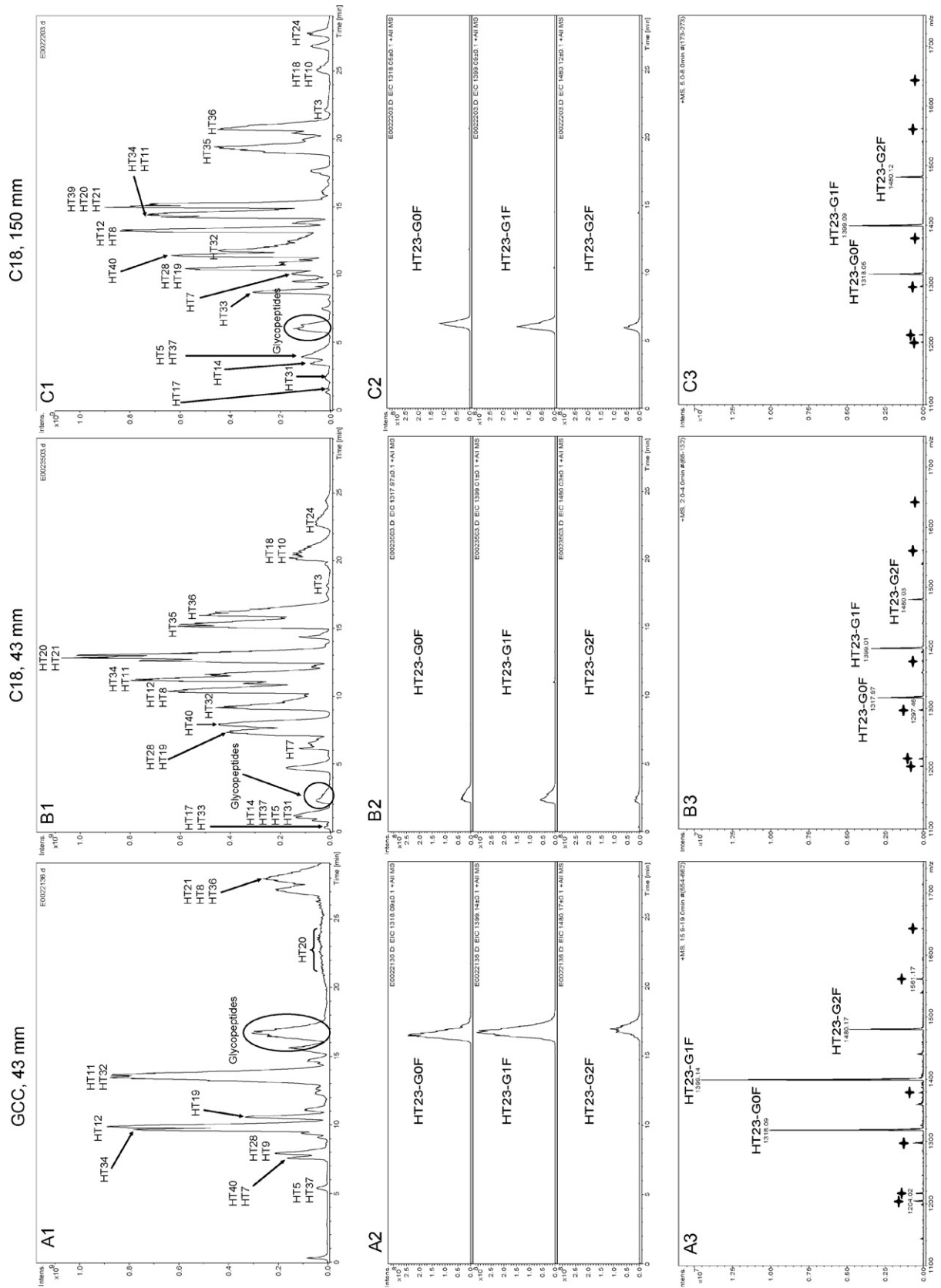
Consequently, those MS/MS experiments performed on the three major released N-glycans of A2CHM, bear evidence of micro-heterogeneities in the glycosylation profile. Indeed, unexpected forms isobaric to G2F were deduced from the fragmentation pattern of the corresponding parent ion. Single mass measurement does not allow discriminating between these isoforms. A high resolution technique such as capillary electrophoresis or capillary electrochromatography [54] might be required in order to separate and quantify them. Additional information regarding carbohydrate linkages would rely on the presence of cross-ring linkage products usually obtained either by fragmentation of methylated derivatives [48] or resulting from high-energetic MS/MS collisions [46].

### 3.3. Tryptic peptide mapping by nanoLC-Chip-MS/MS

The nanoLC-Chip-MS-based approaches have recently been demonstrated in glycomics. Several reviews describe how miniaturization became a general trend in LC-MS of glycoconjugates and glycans [55,56]. Indeed, nanoESI-MS [57], which has been shown as an effective tool for carbohydrate research, presents several limitations such as lack of reproducibility, low sampling throughput and carryovers. Microchip systems can be classified into two categories. First, out of plane devices with hundreds of nanospray emitters, are fully automated chip-based nanoESI robot dedicated to high throughput analysis [56,58,59]. The second category consists of thin plane chips made from glass or polymer material well suited to integration of other analytical processes prior to sample delivery such as sample preparation, purification and separation [60]. Miniaturization of these systems minimizes dead volumes allowing nanoLC-Chip to show better chromatographic performance (reproducibility, peak resolution, peak shape, sensitivity, spray stability) than classical nanoLC systems using 75  $\mu$ m inner diameter columns. The embedding microsyringes are much easier to use than glass nanospray tips, and they provide superior robustness and stability with improved ionization efficiency and sensitivity. Retention and selectivity of classical reversed phase packing materials do not allow good separation of glycopeptides. On the contrary, graphitized carbon chromatography has shown efficient separation of neutral or anionic oligosaccharides and glycopeptides with great stability and long life [61]. The use of nanoLC-Chip-MS packed with graphite material was recently described for separation of oligosaccharides [62,63]. For these reasons, we have used nanoLC-Chip/MS packed with porous graphitized carbon for this glycopeptide study.

In a previous article [28], we reported the glycosylation profile of A2CHM after peptide mapping by RP-HPLC coupled to mass spectrometry. Glycopeptides containing the glycosylated Asn<sup>297</sup> were generated and analyzed after trypsin (-R/EEQYN<sup>297</sup>STYR/V-) or endoproteinase Lys-C cleavage (-K/TKPREEQYN<sup>297</sup>STYRVSVLTVLHQLDGLNGK/E-). Among the peaks corresponding to glycosylated peptides, the three main ones were peptides containing the "G0F", "G1F" and "G2F" forms. Two additional small glycoforms, G2F+ $\alpha$ 1-3 Gal and G2F+2  $\alpha$ 1-3 Gal, were also identified with a 4 and 2% ratio, respectively. For clarity reasons, the tryptic peptide (-R/EEQYN<sup>297</sup>STYR/V-) of the heavy chain will be designated as "HT23" in the following sections of this paper. The associated glycopeptides will thus be called HT23-G0F, HT23-G1F, etc. The nomenclature G0F, G1F and G2F remains used for the glycans themselves.

In the next part of the work, we have performed nanoLC-MS/MS analyses of the peptide mixture resulting from the heavy chain of A2CHM after tryptic digestion using three different nanoLC-Chips: two C18 LC-Chips (43 and 150 mm lengths) and a graphitized carbon LC-Chip (43 mm length).



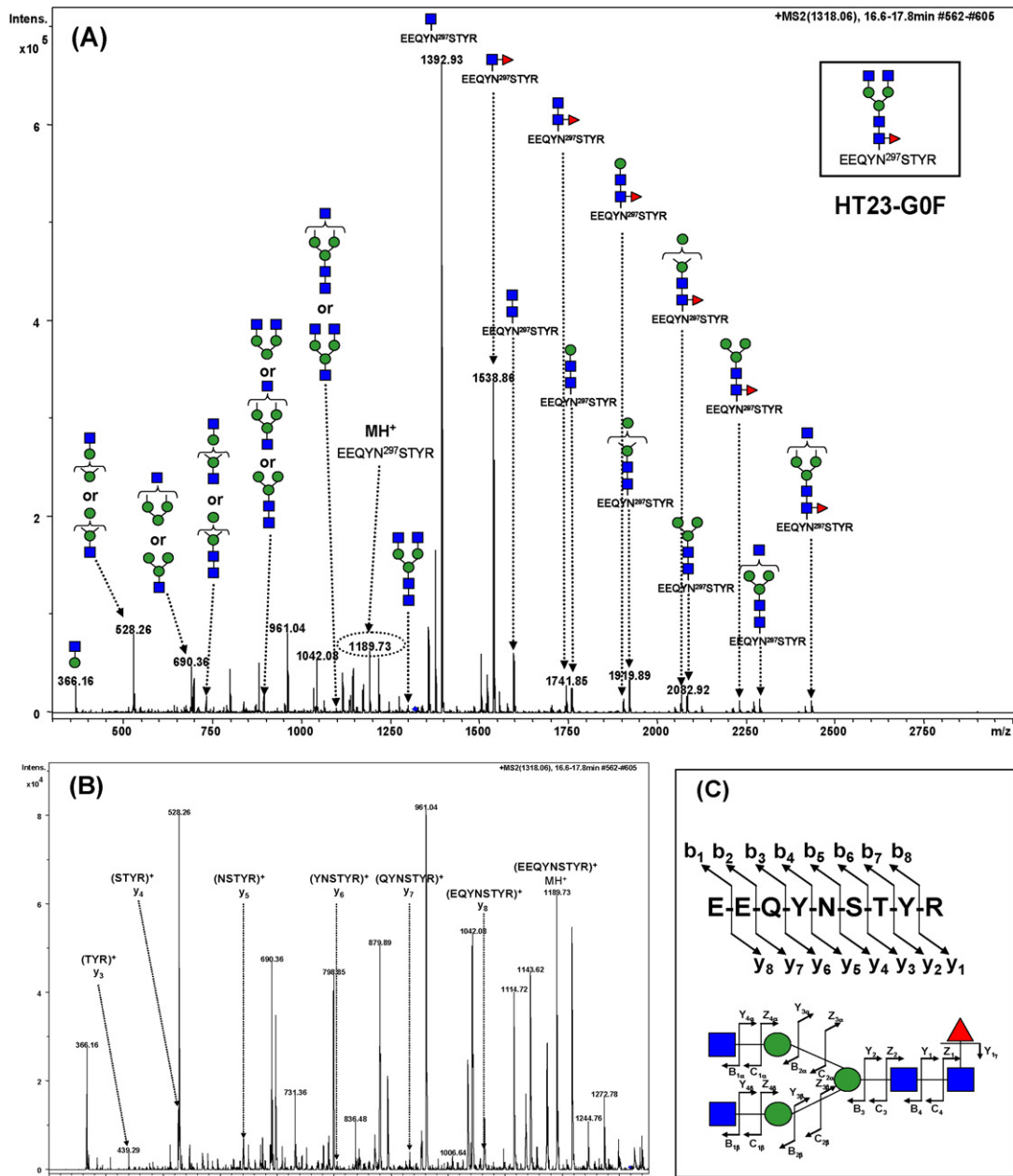
**Fig. 6.** Comparison of the nanoLC–MS analysis performed on a 43 mm graphitized carbon column GCC (A), a 43 mm C18 column (B) and a 150 mm C18 column (C) with respectively, from the top downwards, the annotated base peak chromatograms (A1, B1 and C1), the extracted ion chromatograms of HT23–G0F, HT23–G1F and HT23–G2F (2+) (A2, B2 and C2) and the combined mass spectra corresponding to the area of glycopeptides elution (A3, B3 and C3). Minor glycopeptides observed in the combined mass spectra were labeled by a cross. The same intensity scale has been used for both (A), (B) and (C) conditions in order to be able to compare the results.

### 3.3.1. Reversed phase column versus graphitized carbon column

In a first step, a series of nanoLC–MS experiments were performed on the three types of nanoLC-Chips for comparison of chromatographic performance concerning glycopeptide analysis (Fig. 6A1, B1 and C1). The ion currents corresponding to HT23-G0F, HT23-G1F and HT23-G2F (2+) were extracted showing that glycopeptides were not fully separated whatever was the column (Fig. 6A2, B2 and C2). Glycopeptides were better retained on the graphitized carbon column with retention time ranging from 16 to 19 min compared to RP C18 columns with much shorter retention times (2–8 min). Spectra recorded in the elution time range of glycopeptides were combined resulting in an average mass spectrum, which displayed nine glycoforms for each nanoLC-Chip type (Fig. 6A3, B3 and C3). Even if those spectra were qualitatively identical, the glycopeptide signal was more intense with

the graphitized carbon nanoLC-Chip than with reversed phase columns, which would therefore improve significantly the quality of further MS/MS experiments, especially on minor species. Indeed hydrophilic species are known to be better retained on graphitized carbon phase. The potential glycopeptide losses during the enrichment step on the trapping column are thus less critical for the graphitized carbon LC-Chip than for C18 LC-Chips. Moreover, glycopeptides retained on the graphitized carbon phase are eluted with an higher acetonitrile percentage leading to a better ionization. The slight increase in retention time resulting from the use of a 150 mm column rather than a 43 mm column C18 LC-Chips did not significantly impact on the detection of glycopeptides.

Secondly, the results provided by the three LC-Chip systems were also compared from the point of view of non-glycosylated peptides. Fifteen, 24 and 25 peptides were respectively identified



**Fig. 7.** (A) MS/MS spectrum of the glycopeptide HT23-G0F after nanoLC-Chip ion trap analysis of the tryptic mixture of A2CHM heavy chain. (B) Zoom on the mass range from 300 to 1350  $m/z$  showing peptide and glycan fragmentation. (C) HT23 peptide fragmentation following the nomenclature of Biemann et al. and G0F glycan fragmentation following Domon et al.

on the graphitized carbon, the 43 mm C18 and the 150 mm C18 LC-Chip showing that the reverse phase material was more suitable for the analysis of non-glycosylated species. However, the ion trap mass spectrometer transmission parameters were optimized for the detection of expected glycopeptides, which have higher  $m/z$  values than non-glycosylated peptides. These experimental conditions were therefore significantly different from those we reported in a previous study [28], in which A2CHM heavy chain was analyzed with a 2.1 mm  $\times$  50 mm C18 column allowing the detection of 40 tryptic peptides (i.e. 100% sequence coverage).

In conclusion, the use of graphitized carbon LC-Chip versus C18 column was shown to clearly improve the detection of glycopeptides allowing MS/MS experiments to be undertaken in optimized conditions. We have therefore used this technique for the following nanoLC-Chip–MS/MS study aiming at the characterization of each glycoform, including the minor species.

### 3.3.2. MS/MS experiments: glycoforms characterization

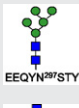
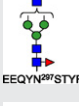
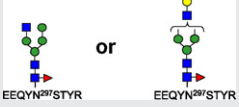
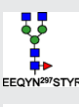
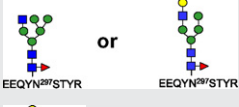
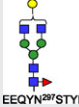

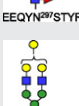
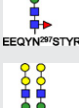
For the nanoLC-Chip–MS/MS analysis of A2CHM heavy chain tryptic peptide mixture, a list of masses was set in order to automatically isolate and fragment the doubly protonated ion of each of the nine detected glycopeptides. Looking at the tandem mass spectra of glycopeptides, we observed predominantly fragment ions resulting from the fragmentation of glycosidic bonds as already described [64]. Ions corresponding to the fragmentation of the peptide backbone were much less intense and, for some cases, it was possible to observe fragment ions corresponding to y- and b-types ions of the peptide backbone [65].

As an example, the MS/MS spectrum of HT23–G0F is shown in Fig. 7. The doubly charged molecular ion at  $m/z$  1318.06 displayed a series of intense, single protonated ion fragments (Fig. 7A). As previously mentioned, most of the fragments corresponded to successive neutral sugar losses. Two fragmentation pathways were observed. One consisted of ions, which conserved the core-fucosyl region intact and lost successively neutral sugars ( $m/z$  1538.86, 1741.85, 1903.90, 2065.95, 2228.05 and 2431.08). The second one consisted in ions, which lost the core-fucose plus additional monosaccharides (ions at  $m/z$  1392.93, 1596.01, 1758.06, 1919.89, 2082.16, 2285.24). The combination of both types of information allowed us to ascertain the structure of the N-linked glycan. In addition, we observed in the low  $m/z$  range, ions corresponding to Y and B glycan backbone fragments and to internal glycan fragments according to the nomenclature of Domon and Costello [52]. For example, ions at  $m/z$  366.16 and 528.26 which were identified respectively as [Hex + HexNAc + H]<sup>+</sup> and [2Hex + HexNAc + H]<sup>+</sup> are fragments typically observed in MS/MS spectra of N-glycans and associated glycopeptides. These ions do not give information about the glycan structure itself. Nevertheless they are referred to diagnostic ions useful to assign glycopeptides in complex mixtures [65]. Moreover, the MS/MS spectrum presented a single protonated ion at  $m/z$  1189.73 corresponding to the mass of peptide HT23 without glycosylation. A zoom on the low mass range of the MS/MS spectrum is presented Fig. 7B. In this area, we observed low intense y-type ions of this peptide at  $m/z$  439.29, 526.32, 640.36, 803.42, 931.48 and 1060.52 (respectively fragments  $y_3$  to  $y_8$  according to the nomenclature of Biemann [66]) (Fig. 7C). Finally, the whole MS/MS spectrum provided information at several levels: regarding the position of the N-glycosylation (ascertained in position Asn<sup>297</sup>), the peptide amino acid sequence itself and the structure of the N-linked glycan G0F.

Table 3 summarizes the nine studied glycoforms and their associated structures. MS/MS spectra of glycopeptides at  $m/z$  1399.14 and 1480.17 (respectively HT23–G1F and so called HT23–G2F, data not shown) presented the same fragmentation pattern as for HT23–

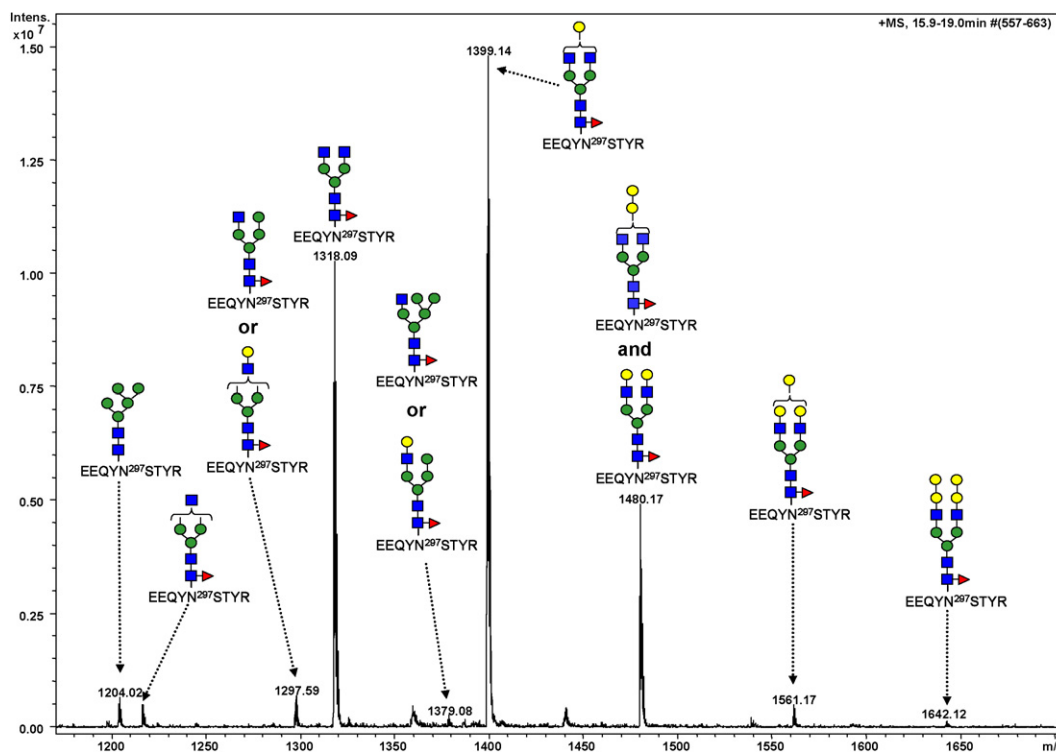
**Table 3**

Summary of glycoforms assigned to the doubly protonated ions observed with their respective ratios calculated from averaged mass spectrum

Ions observed ( $m/z$ )	Glycoform structures	Ratios (%)
1204.02		2.0
1216.54		1.5
1297.59		2.1
1318.09		31.4
1379.08		0.9
1399.14		45.2
1480.17		15.0
1561.17		1.5
1642.12		0.4

G0F. However, the MS/MS spectrum of the glycopeptide at  $m/z$  1480.17, displayed an ion at  $m/z$  2756.36 which could not be attributed to a HT23–G2F fragment, but which corresponds to the mass of HT23–G2F with a GlcNAc loss (mass shift of  $-203$  Da). As previously discussed in Section 3.2 (MS/MS spectra of released N-glycans), it may correspond to an isomeric form to G2F which is a G1F +  $\alpha$ 1-3 Gal form. On the MS/MS spectra of the less intense glycopeptides at  $m/z$  1204.02, 1216.54, 1561.17 and 1642.23 (data not shown) only ions resulting from the fragmentation of the glycan backbone were observed. Whereas, the ion at  $m/z$  1189.73 (HT23) was detected in every nine MS/MS spectra, associated b and y series were probably too weak to be measured. The glycopeptides at  $m/z$  1561.17 and 1642.12 could be unambiguously interpreted as G2F +  $\alpha$ 1-3 Gal and G2F + 2  $\alpha$ 1-3 Gal glycoforms. Ions at  $m/z$  1204.02 and 1216.54 were attributed to oligomannose Man<sub>5</sub>GlcNAc<sub>2</sub> and GlcNAcMan<sub>3</sub>GlcNAc<sub>2</sub>Fuc, respectively.

Concerning the glycopeptides at  $m/z$  1297.59 and 1379.08, we could precisely identify the core-fucosyl moiety Man<sub>3</sub>GlcNAc<sub>2</sub>Fuc but we could not completely assess the remaining part of the N-linked glycan. Two structures can be proposed for the glycan part of the peptide at  $m/z$  1297.59 (GalGlcNAcMan<sub>3</sub>GlcNAc<sub>2</sub>Fuc or GlcNAcMan<sub>4</sub>GlcNAc<sub>2</sub>Fuc), however they could not be



**Fig. 8.** Average mass spectrum in the area of elution of glycopeptides after nanoLC-Chip ion trap analysis with a 43 mm length graphitized column (zoom of Fig. 6A3). Nine glycopeptides corresponding to 12 potential glycoforms of A2CHM were detected and further fragmented by MS/MS.

further differentiated. Similarly the N-linked glycan corresponding to the glycopeptide at  $m/z$  1379.08 could be either GalGlcNAcMan<sub>4</sub>GlcNAc<sub>2</sub>Fuc or GlcNAcMan<sub>5</sub>GlcNAc<sub>2</sub>Fuc (see Table 3).

As previously discussed in Section 3.2, 4 out of the 12 proposed structures are low abundant hybrid type or oligomannosidic N-glycans that result from an incomplete glycan maturation process in cells.

### 3.3.3. Study of glycoforms heterogeneity

A quantification of glycopeptides was performed based on their relative intensity from the combined mass spectrum presented in Fig. 8. Indeed as all glycopeptides have a similar structure (each glycan is N-linked to the same HT23 peptide), we assumed that their response factors would be very close. We observed the five glycoforms previously described by a more classical LC-MS approach [28] with the following ratios: HT23-G0F (31.4%), HT23-G1F (45.2%), HT23-G2F (15.0%), HT23-G2F+ $\alpha$ 1-3 Gal (1.5%) and HT23-G2F+2  $\alpha$ 1-3 Gal (0.4%).

Furthermore, we characterized four additional glycopeptides, which were not identified by our previously mentioned approach. The HT23-GlcNAcMan<sub>3</sub>GlcNAc<sub>2</sub>Fuc form ( $m/z$  1216.5) and the oligomannosidic HT23-Man<sub>5</sub>GlcNAc<sub>2</sub> ( $m/z$  1204.02) were detected with a 1.5 and 2.0% ratio, respectively. Species at  $m/z$  1297.59 and 1379.08 contributed respectively to 2.1 and 0.9% of the total amount of glycopeptides.

NanoLC-Chip-MS/MS analyses of glycopeptides using graphitized carbon as stationary phase have shown their significance. Low glycopeptide loss during the enrichment step, good retention and good separation of glycopeptides from other peptides, allowed improvement in the detection of minor glycoforms and provided high MS/MS quality. We have been able to characterize at least nine glycoforms reflecting the micro-heterogeneities of the monoclonal antibody.

## 4. Discussion

The top-down MS-approach by LC-ESI-TOF, performed on intact MAb, allows direct and fast mass measurements without prior tedious sample preparation. The method provides in one-shot masses of  $\approx$ 150 kDa weight glycoforms in heterogeneous mixtures with accuracy lower than 100 ppm permitting a preliminary global characterization of the antibody. Due to the asymmetry of heavy chain glycosylation, the analysis of intact MAb results in spectra showing the highly complex combination of glycoforms on the two sites without any possible detailed characterization of each site. A method to decrease this complexity is to perform the analysis of reduced MAb. Then a higher resolution will be obtained allowing a relative quantification of each heavy chain glycoform. Still, LC-ESI-TOF on intact or reduced MAb remains a rough approach, informative about the integrity of the whole antibody, but which does not allow detailed structural characterization.

The second approach – ESI-MS/MS direct analysis of released N-linked glycans – has been exhaustively used by many groups and was applied in this study for the fine characterization of the most abundant carbohydrates reported for MAb, the so-called G0F, G1F and G2F glycoforms. Using this strategy we confirmed unambiguously the overall composition and structure of these core fucosylated bi-antennary species, faster than using sequential digestion with selective exoglycosidases followed by normal-phase-high performance liquid chromatography [68]. Moreover, we show evidence for isobaric forms of G2F, which correspond in part to low abundant, hybrid glycans. The limitations of the approach remain in the lack of information regarding carbohydrate linkages and anomery. This was neither displayed by the other methods used and could be partially circumvented by an appropriate derivation of N-glycans. The deglycosylation step can also be limiting for the identification of some glycoforms. Indeed, PNGaseF cleaves between the innermost GlcNAc and asparagine residues of high

mannose, hybrid and complex oligosaccharides from N-linked glycoproteins but does not cleave N-linked glycans containing core  $\alpha$ -1,3 fucose for example [67]. Unlike mammalian expression systems, which produce only fucose  $\alpha$ -1,6, plants usually contain fucose  $\alpha$ -1,3 linked to the first core GlcNAc residue of the N-glycans. Different transgenic plants or the use of moss or aquatic plants in bioreactors have been proposed in the recent years as expression system for therapeutics as been observed in recent years, offering several advantages in terms of safety and cost-of-goods [17]. Thus, a more versatile method for characterization of MAb glycosylation must exclude an endoglycosidase digestion step in order to avoid the introduction of a bias during the analysis. Indeed, released N-glycans mixtures after hydrolysis may not be the exact picture of the MAb glycosylation profile. Moreover, additional experimental steps aiming at the separation and purification of N-glycans from their protein moieties contribute to the loss of minor sugar species easily absorbed on surfaces during sample preparation. Therefore, lack of sensitivity to detect low abundant glycoforms could be a bottleneck for such an approach.

With the last strategy, we have analyzed by nanoLC-Chip-MS/MS glycopeptides resulting from the heavy chain tryptic digestion. The approach was shown to be valuable from several points of view. First, integration of multiple steps in a single chip combined to miniaturization in terms of column dimensions, flow rates and surface area that glycopeptide samples encounter, significantly improves the sensitivity for low abundant species detection. As reported here, we were able to detect more glycoforms than we did previously with a more conventional LC-MS peptide mapping strategy [28]. Secondly, results were better than those obtained with the two other approaches described in this paper. Very informative MS/MS spectra were obtained on glycopeptides since they provide complete structure of the N-glycans (composition and linear sequence) plus additional information regarding the glycopeptide amino acid sequence. It is seldom possible to obtain both types of information within a single MS/MS spectrum. This may depend on the nature of the glycopeptides but is interesting to show that in the present case study, both type of fragmentation were clearly observed. As expected, the selectivity of carbon graphite stationary phase appeared well suited to address analysis of glycopeptides. It provides better retention and sensitivity than C18 material. In a global and complete structural investigation of MAbs the corresponding tryptic mixture could be split in two parts to be analyzed by reversed phase and carbon graphite chromatography. Taking advantage of the short gradient offered by the chip technology it would not extend the analysis duration and would provide a systematic and complete characterization by MS/MS of the whole antibody sequence including its potential modifications.

## 5. Conclusion

We have evaluated the efficacy of three level MS-based strategies to characterize MAb glycosylation of a murine and of a humanized antibody, produced in NS0 and CHO cells, the two mostly used production system for therapeutic immunoglobulins. Beyond the RP-HPLC-TOF approach, now commonly used to assess MAbs modifications with minimal sample preparation, a new nanoLC-Chip-MS/MS bottom-up strategy is proposed. As a proof-of-concept, the methodology was applied to the elucidation of an NS0-produced antibody structure, which exhibits more glycoforms than CHO-produced MAbs. Interestingly, nine species of various relative abundances were detected, characterized by MS/MS and interpreted as corresponding to 12 glycoform structures. This nanoLC-Chip-MS/MS method can be implemented as an efficient and fast tool to routinely screen monoclonal antibody production during discovery and selection of the best clone, and also

to screen antibody batch-to-batch consistency, during the pharmaceutical development and scaling-up.

Furthermore, the method described herein will also be useful to characterize antibodies produced in alternative systems (human cell lines, yeasts, insect cells/baculoviruses, transgenic animals and plants, chicken eggs, moss, etc.) to assess low levels of immunogenic carbohydrates as well as for the next-generation of glyco-engineered antibodies with improved effector functions (ADCC, CDC), plasmatic half life and humanized glycosylation [68].

## Acknowledgments

The authors thank Dr. Christian Bailly for his support for this project, Dr. Peter Lowe for a careful reading of the manuscript and Mrs. Claire Catry for valuable technical assistance.

## References

- [1] P.J. Carter, *Nat. Rev. Immunol.* 6 (2006) 343.
- [2] I. Kola, J. Landis, *Nat. Rev. Drug Discov.* 3 (2004) 711.
- [3] J.M. Reichert, C.J. Rosensweig, L.B. Faden, M.C. Dewitz, *Nat. Biotechnol.* 23 (2005) 1073.
- [4] N. Takahashi, I. Ishii, H. Ishihara, M. Mori, S. Tejima, R. Jefferis, S. Endo, Y. Arata, *Biochemistry* 26 (1987) 1137.
- [5] P.M. Rudd, R.J. Leatherbarrow, T.W. Rademacher, R.A. Dwek, *Mol. Immunol.* 28 (1991) 1369.
- [6] R. Jefferis, *Biotechnol. Prog.* 21 (2005) 11.
- [7] R. Jefferis, *Adv. Exp. Med. Biol.* 564 (2005) 143.
- [8] L. Huang, C.E. Mitchell, *Methods Mol. Biol.* 308 (2005) 411.
- [9] R. Jefferis, in: W. Swaby (Ed.), *Bioprocessing & Biopartnering*, Touch Briefings, 2006, p. 36.
- [10] T.S. Raju, J.B. Briggs, S.M. Borge, A.J. Jones, *Glycobiology* 10 (2000) 477.
- [11] S. Narasimhan, *J. Biol. Chem.* 257 (1982) 10235.
- [12] M.R. Wormald, P.M. Rudd, D.J. Harvey, S.C. Chang, I.G. Scragg, R.A. Dwek, *Biochemistry* 36 (1997) 1370.
- [13] J.N. Arnold, M.R. Wormald, R.B. Sim, P.M. Rudd, R.A. Dwek, *Annu. Rev. Immunol.* 25 (2007) 21.
- [14] Y. Kaneko, F. Nimmerjahn, J.V. Ravetch, *Science* 313 (2006) 670.
- [15] T. Shinkawa, K. Nakamura, N. Yamane, E. Shoji-Hosaka, Y. Kanda, M. Sakurada, K. Uchida, H. Anazawa, M. Satoh, M. Yamasaki, N. Hanai, K. Shitara, *J. Biol. Chem.* 278 (2003) 3466.
- [16] T.S. Raju, J.B. Briggs, S.M. Chamow, M.E. Winkler, A.J. Jones, *Biochemistry* 40 (2001) 8868.
- [17] K.M. Cox, J.D. Sterling, J.T. Regan, J.R. Gasdaska, K.K. Frantz, C.G. Peele, A. Black, D. Passmore, C. Moldovan-Loomis, M. Srinivasan, S. Cuison, P.M. Cardarelli, L.F. Dickey, *Nat. Biotechnol.* 24 (2006) 1591.
- [18] R. Niwa, A. Natsume, A. Uehara, M. Wakitani, S. Iida, K. Uchida, M. Satoh, K. Shitara, *J. Immunol. Methods* 306 (2005) 151.
- [19] Y. Kanda, N. Yamane-Ohnuki, N. Sakai, K. Yamano, R. Nakano, M. Inoue, H. Misaka, S. Iida, M. Wakitani, Y. Konno, K. Yano, K. Shitara, S. Hosoi, M. Satoh, *Biotechnol. Bioeng.* 94 (2006) 680.
- [20] L. Zhu, M.C. Van de Lavoie, J. Albanese, D.O. Beenhouwer, P.M. Cardarelli, S. Cuison, D.F. Deng, S. Deshpande, J.H. Diamond, L. Green, E.L. Halk, B.S. Heyer, R.M. Kay, A. Kerchner, P.A. Leighton, C.M. Mather, S.L. Morrison, Z.L. Nikolov, D.B. Passmore, A. Pradas-Monne, B.T. Preston, V.S. Rangan, M. Shi, M. Srinivasan, S.G. White, P. Winters-Digiaco, S. Wong, W. Zhou, R.J. Etches, *Nat. Biotechnol.* 23 (2005) 1159.
- [21] J.P. Kunkel, D.C. Jan, M. Butler, J.C. Jamieson, *Biotechnol. Prog.* 16 (2000) 462.
- [22] C.A. Srebalus Barnes, A. Lim, *Mass Spectrom. Rev.* 26 (2007) 370.
- [23] A. Dell, H.R. Morris, *Science* 291 (2001) 2351.
- [24] Y. Mechref, M.V. Novotny, *Chem. Rev.* 102 (2002) 321.
- [25] J. Qian, T. Liu, L. Yang, A. Daus, R. Crowley, Q. Zhou, *Anal. Biochem.* 364 (2007) 8.
- [26] J.A. Saba, J.P. Kunkel, D.C. Jan, W.E. Ens, K.G. Standing, M. Butler, J.C. Jamieson, H. Perreault, *Anal. Biochem.* 305 (2002) 16.
- [27] Y. Mechref, J. Muzikar, M.V. Novotny, *Electrophoresis* 26 (2005) 2034.
- [28] A. Beck, M.C. Bussat, N. Zorn, V. Robillard, C. Klinguer-Hamour, S. Chenu, L. Goetsch, N. Corvaia, A. Van Dorsselaer, J.F. Haeuw, *J. Chromatogr. B Anal. Technol. Biomed. Life Sci.* 819 (2005) 203.
- [29] T.M. Dillon, P.V. Bondarenko, R.M. Speed, *J. Chromatogr. A* 1053 (2004) 299.
- [30] T.M. Dillon, P.V. Bondarenko, D.S. Rehder, G.D. Pipes, G.R. Kleemann, M.S. Ricci, *J. Chromatogr. A* 1120 (2006) 112.
- [31] D.S. Rehder, T.M. Dillon, G.D. Pipes, P.V. Bondarenko, *J. Chromatogr. A* 1102 (2006) 164.
- [32] Y. Lyubarskaya, D. Houde, J. Woodard, D. Murphy, R. Mhatre, *Anal. Biochem.* 348 (2006) 24.
- [33] J. Siemiakoski, Y. Lyubarskaya, D. Houde, S. Tep, R. Mhatre, *Carbohydr. Res.* 341 (2006) 410.

- [34] H.S. Gadgil, G.D. Pipes, T.M. Dillon, M.J. Treuheit, P.V. Bondarenko, *J. Am. Soc. Mass Spectrom.* 17 (2006) 867.
- [35] L. Wang, G. Amphlett, J.M. Lambert, W. Blattler, W. Zhang, *Pharmaceut. Res.* 22 (2005) 1338.
- [36] B. Yan, J. Valliere-Douglass, L. Brady, S. Steen, M. Han, D. Pace, S. Elliott, Z. Yates, Y. Han, A. Balland, W. Wang, D. Pettit, *J. Chromatogr. A* 1164 (2007) 153.
- [37] L. Yu, R.L. Remmele Jr., B. He, *Rapid Commun. Mass Spectrom.* 20 (2006) 3674.
- [38] D. Chelius, K. Jing, A. Lueras, D.S. Rehder, T.M. Dillon, A. Vizel, R.S. Rajan, T. Li, M.J. Treuheit, P.V. Bondarenko, *Anal. Chem.* 78 (2006) 2370.
- [39] J. Yang, S. Wang, J. Liu, A. Raghani, *J. Chromatogr. A* 1156 (2007) 174.
- [40] L. Presta, *Curr. Opin. Struct. Biol.* 13 (2003) 519.
- [41] A.E. Hills, A. Patel, P. Boyd, D.C. James, *Biotechnol. Bioeng.* 75 (2001) 239.
- [42] M. Perkins, R. Theiler, S. Lunte, M. Jeschke, *Pharmaceut. Res.* 17 (2000) 1110.
- [43] R.J. Harris, *Dev. Biol. (Basel)* 122 (2005) 117.
- [44] C. Quan, E. Alcala, I. Petkovska, D. Matthews, E. Canova-Davis, R. Taticek, S. Ma, *Anal. Biochem.* 373 (2008) 179.
- [45] A. Beck, C. Klinguer-Hamour, M.C. Bussat, T. Champion, J.F. Haeuw, L. Goetsch, T. Wurch, M. Sugawara, A. Milon, A. Van Dorsseleer, T. Nguyen, N. Corvaia, *J. Pept. Sci.* 13 (2007) 588.
- [46] V.N. Reinhold, B.B. Reinhold, C.E. Costello, *Anal. Chem.* 67 (1995) 1772.
- [47] A.S. Weiskopf, P. Vouros, D.J. Harvey, *Anal. Chem.* 70 (1998) 4441.
- [48] D.M. Sheeley, V.N. Reinhold, *Anal. Chem.* 70 (1998) 3053.
- [49] D.J. Harvey, *J. Mass Spectrom.* 35 (2000) 1178.
- [50] K.R. Anumula, *Anal. Biochem.* 283 (2000) 17.
- [51] E. Wagner, PhD thesis, Université Louis Pasteur (Strasbourg, Fr), 2004.
- [52] B. Domon, C.E. Costello, *Glycoconjugate J.* 5 (1988) 397.
- [53] K. Barbin, J. Stieglmaier, D. Saul, K. Stieglmaier, B. Stockmeyer, M. Pfeiffer, P. Lang, G.H. Fey, *J. Immunother.* 29 (2006) 122.
- [54] A.H. Que, M.V. Novotny, *Anal. Bioanal. Chem.* 375 (2003) 599.
- [55] Y. Mechref, M.V. Novotny, *J. Chromatogr. B Anal. Technol. Biomed. Life Sci.* 841 (2006) 65.
- [56] A. Zamfir, S. Vakhrushev, A. Sterling, H.J. Niebel, M. Allen, J. Peter-Katalinic, *Anal. Chem.* 76 (2004) 2046.
- [57] M. Wilm, M. Mann, *Anal. Chem.* 68 (1996) 1.
- [58] S. Zhang, D. Chelius, *J. Biomol. Tech.* 15 (2004) 120.
- [59] A.D. Zamfir, L. Bindila, N. Lion, M. Allen, H.H. Girault, J. Peter-Katalinic, *Electrophoresis* 26 (2005) 3650.
- [60] H. Yin, K. Killeen, R. Brennen, D. Sobek, M. Werlich, G.T. van de, *Anal. Chem.* 77 (2005) 527.
- [61] M.J. Davies, K.D. Smith, R.A. Carruthers, W. Chai, A.M. Lawson, E.F. Hounsell, *J. Chromatogr.* 646 (1993) 317.
- [62] M. Ninonuevo, H. An, H. Yin, K. Killeen, R. Grimm, R. Ward, B. German, C. Lebrilla, *Electrophoresis* 26 (2005) 3641.
- [63] M.R. Ninonuevo, Y. Park, H. Yin, J. Zhang, R.E. Ward, B.H. Clowers, J.B. German, S.L. Freeman, K. Killeen, R. Grimm, C.B. Lebrilla, *J. Agric. Food Chem.* 54 (2006) 7471.
- [64] U.M. Demelbauer, M. Zehl, A. Plemat, G. Allmaier, A. Rizzi, *Rapid Commun. Mass Spectrom.* 18 (2004) 1575.
- [65] M. Wuhrer, M.I. Catalina, A.M. Deelder, C.H. Hokke, *J. Chromatogr. B Anal. Technol. Biomed. Life Sci.* 849 (2007) 115.
- [66] K. Biemann, *Annu. Rev. Biochem.* 61 (1992) 977.
- [67] F. Maley, R.B. Trimble, A.L. Tarentino, T.H. Plummer Jr., *Anal. Biochem.* 180 (1989) 195.
- [68] A. Beck, E. Wagner-Rousset, M.C. Bussat, M. Lokteff, C. Klinguer-Hamour, J.F. Haeuw, L. Goetsch, T. Wurch, A. Van Dorsseleer, N. Corvaia, *Current Pharm. Biotechnol.* (2008), in press.